

Development of Super High Resolution Global and Regional Climate Models

Project Representative

Akira Noda Meteorological Research Institute

Authors

Akira Noda ^{*1}, Shoji Kusunoki ^{*1} and Masaomi Nakamura ^{*1}

^{*1} Meteorological Research Institute

Under the Kyosei4 Project funded by the Ministry of Education, Culture, Science and Technology (MEXT), unprecedented high resolution global and regional climate models were developed on the Earth Simulator to investigate the global warming on tropical cyclones, the Baiu frontal rain band and heavy rainfalls which cannot be resolved in conventional climate models.

Time-slice experiments were performed using an atmospheric general circulation model (AGCM) with a 20-km grid resolution by prescribing sea surface temperature (SST) as boundary conditions. The SST data were obtained from observation and IPCC AR4 global warming simulations with the MRI-CGCM2.3.2 and the MIROC3.2 (hires). The experiments show that the global number of tropical cyclones (TCs) decreases by about 30% in a warmer climate in spite of a large difference in global mean SST increase between the models. However, the change in regional TC frequency is found to be sensitive to local SST changes. In the rainy season, Baiu, over East Asia in summer, precipitation consistently increases over the Yangtze River valley, the East China Sea, and the ocean to the south of the Japan archipelago. It is also found robust that the termination of the Baiu season tends to be delayed until August.

Non-hydrostatic models nested in the 20-km AGCM were developed to simulate the heavy rainfalls in the Baiu season around Japan with a horizontal grid size of 5km for 10 years in both the present and future global warming climates. It is shown that due to the global warming the precipitation amount is projected to increase except eastern and northern Japan, the rates of increase are larger with more intense precipitations, and the return values of extreme precipitations become larger. Furthermore, simulations with a grid size of 1km were executed to simulate a more detailed structure of precipitation and to study the effects of resolution. It is found that 1km-NHM improves 5km-NHM results in producing more realistically the precipitation-frequency spectrum against precipitation intensity and organization of precipitation system followed by heavy rainfall.

Keywords: global warming projection, high resolution global model, non-hydrostatic cloud resolving model, tropical cyclone, Baiu

1. Subproject 1: Development of a global climate model with a horizontal resolution of 20 km

1.1 Models and experimental design

Global warming projections with a 20-km mesh global atmospheric general circulation model (AGCM) were conducted by adopting so-called the "time-slice" method (Bengtsson et al. 1996; IPCC 2001). This method is defined as the two-tier global warming projection approach using an atmospheric ocean general circulation model (AOGCM) and an AGCM whose horizontal resolution is much higher than that of atmospheric part of the AOGCM. The experimental designs and names are summarized in Table 1. The present time-slice experiments consist of four runs (AT, AJ, AM, AX) with different sea surface temperature (SST) fields used as the surface boundary condition. The AT and AJ runs are

forced with observed historical and climatological SSTs, respectively. The AM and AJ runs are forced with the SSTs of coupled atmosphere ocean GCMs, the MRI-CGCM2.3.2 (Yukimoto et al. 2006) and the MIROC (hires), respectively. The future time-slice experiments consist of four runs (AK, AN, AS, AY) assuming the IPCC SRES A1B emission scenario. The AK and AM runs are forced with the SSTs of MRI-CGCM2.3.2, whereas the AS and AY runs are forced with the SSTs of MIROC (hires). All the experiments can be classified into two types; those with year-to-year SST variability (AT, AM, AN, AX, AY) and those without year-to-year SST variability (AJ, AK, AS).

Table 1 Experimental design.

(a) Present climate

Name	Sea Surface Temperature (SST)			integration time (year)
	Type	Period	Year-to-year variability	
AT	Observation, AMIP run	Jan 1979 to Feb 2006	Yes	27
AJ	Observed climatology	12 year mean from an 1982 to Dec 1993	No	20
AM	MRI-CGCM2.3.2	Jan 1979 to Dec 1998	Yes	20
AX	MIROC(hires)	20 year mean from Jan 1979 to Dec 1998	No	5

(b) Future climate

Name	Sea Surface Temperature (SST)			integration time (year)
	Type	Period	Year-to-year variability	
AK	Observed climatology + Change projected by MRI-CGCM2.3.2	about year 2090	No	20
AS	Observed climatology + Change projected by MIROC(hires)	about year 2090	No	10
AN	MRI-CGCM2.3.2	Jan 2080 to Dec 2099	Yes	20
AY	MIROC(hires)	20 year mean from Jan 2080 to Dec 2099	No	5

SST change = (year 2080–2099 mean) minus (year 1979–1998 mean)

1.2 Tropical cyclone

We have performed an objective tracking of tropical cyclones (TCs) in the model outputs, basically following the criteria used in previous studies (e.g., Sugi et al. 2002). In addition to our earlier studies, we have investigated sensitivity of the TC climatology to SST conditions in present-day and future climate simulations (see Table 1).

Figure 1 shows TC tracks of the observational data and in a present-day simulation (AT: AMIP experiment with year-to-year variability in the sea surface temperature condition). The geographical distribution of simulated TCs is generally similar to that of the observation. The annual-mean numbers of TCs in present-day and future simulations are shown in Fig. 2. The global and hemispheric numbers of TCs in the model are reduced significantly in all of the future experiments, and the results strengthen our previous findings (e.g., Oouchi et al. 2006). In the Western North Pacific Ocean, the regional number of TCs decreases in the future experiments AK and AY, whereas it increases in another future

experiment AS. The same SST from an AOGCM experiment (MIROC(hires)) is used in a different way between experiments AS and AY as described in Table 1. This suggests that consistent changes in the basin-scale number of TCs could be meaningfully simulated if SST conditions are properly set and consistency between AGCM and AOGCM is carefully checked.

We have also examined TC intensities, in terms of maximum surface wind speed, in the present-day and future simulations. Figure 3 indicates that frequency of intense TCs (e.g., wind speed > 50 m/s) increases globally in the future experiments. The global-mean warming of SST was 1.6 K for the AK experiment and 3.2 K for the AS and AY experiments, respectively. The intensification of simulated TCs is significantly larger in the experiments AS and AY, and this should reflect the difference in the magnitude of global warming. These results indicate robustness of our previous results (Oouchi et al. 2006).

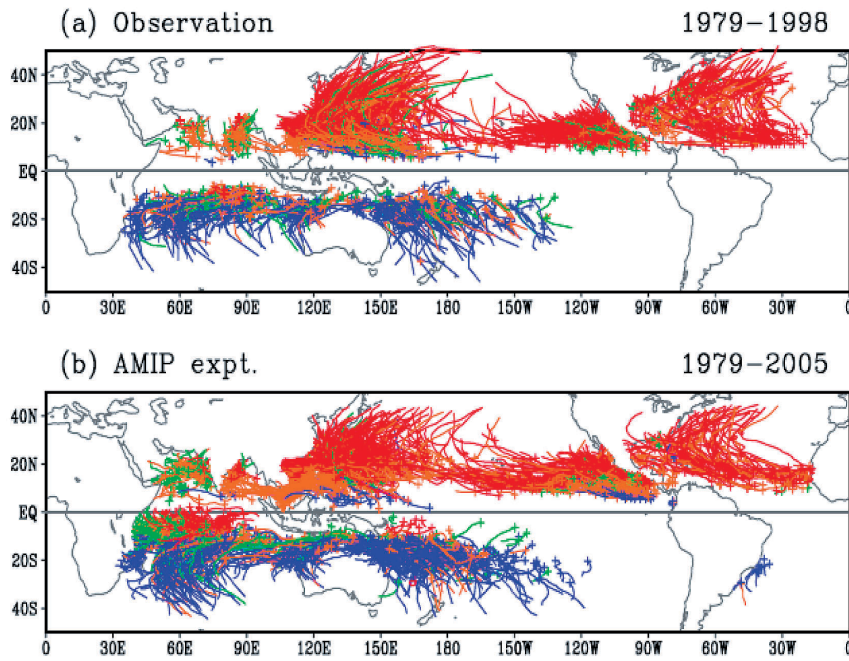


Fig. 1 Tropical cyclone tracks of (a) observational data and (b) AMIP present-day experiment. The tracks detected at different seasons of each year are shown in different colors (blue for January, February and March; green for April, May and June; red for July, August and September; orange for October, November and December).

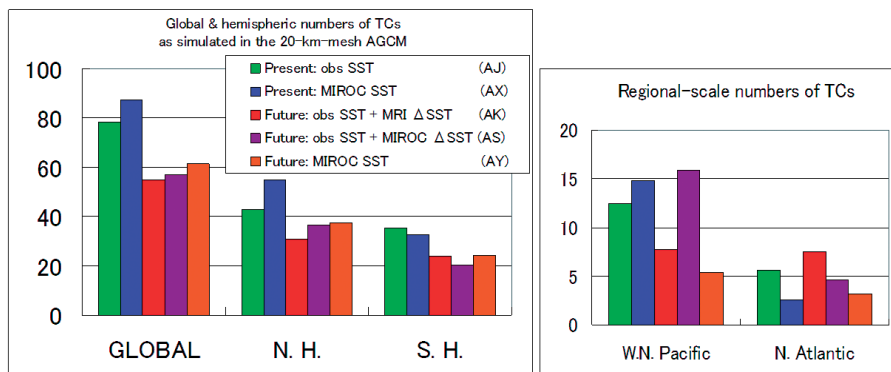


Fig. 2 Annual-mean number of simulated TC formation in the globe, the Northern and Southern Hemispheres (left), and the Western North Pacific and the North Atlantic (right).

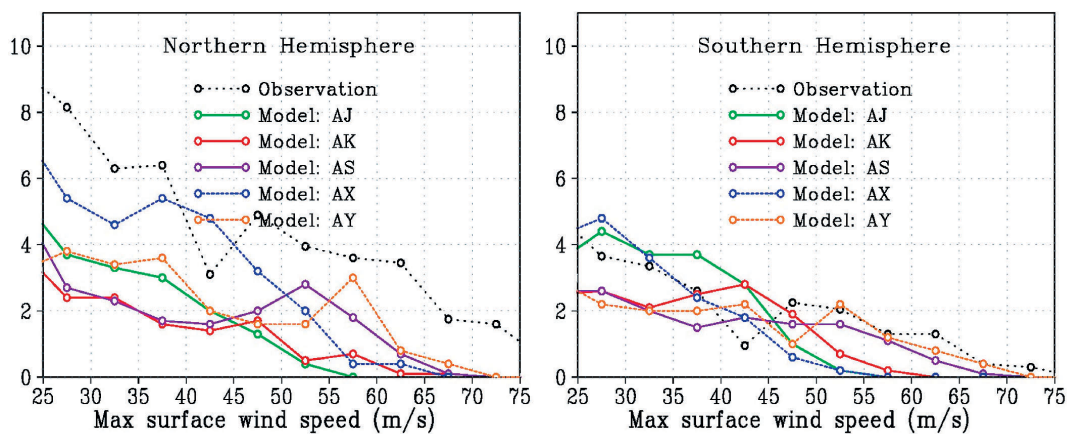


Fig. 3 Frequency distribution of TCs in the Northern and Southern Hemispheres shown as a function of maximum wind speed. The abscissa denotes the peak intensity (maximum surface wind speed), attained in the lifetime of each TC, and the ordinate denotes the annual-mean number of TCs.

1.3 Baiu

Figure 4 shows the geographical distribution of climatological precipitation for July. In the AJ run (b), the model well simulates the observed present climatology (a). In the AM run (c), the model underestimates the observed rainfall amount over Japan. On the contrary, the AX run (d) overestimates rainfall over Japan. These defects are partly due to the discrepancy between simulated SST by AOGCMs and the observed SST. As for the future climate change, precipitation consistently increases over the Yangtze River valley,

the East China Sea, and the ocean to the south of the Japan archipelago (e-f). In contrast, the change of precipitation over Korea, the Japan Sea, and Northern Japan differs among the experiments.

Figure 5 shows the seasonal march of precipitation over the Japan region. In the AJ run (b), the model well simulates the observed northward migration of the Baiu rain band. In the AM run (c), the model also simulates the observed northward migration of the Baiu rain band, although the model underestimates the observed rainfall amount. In the AX run

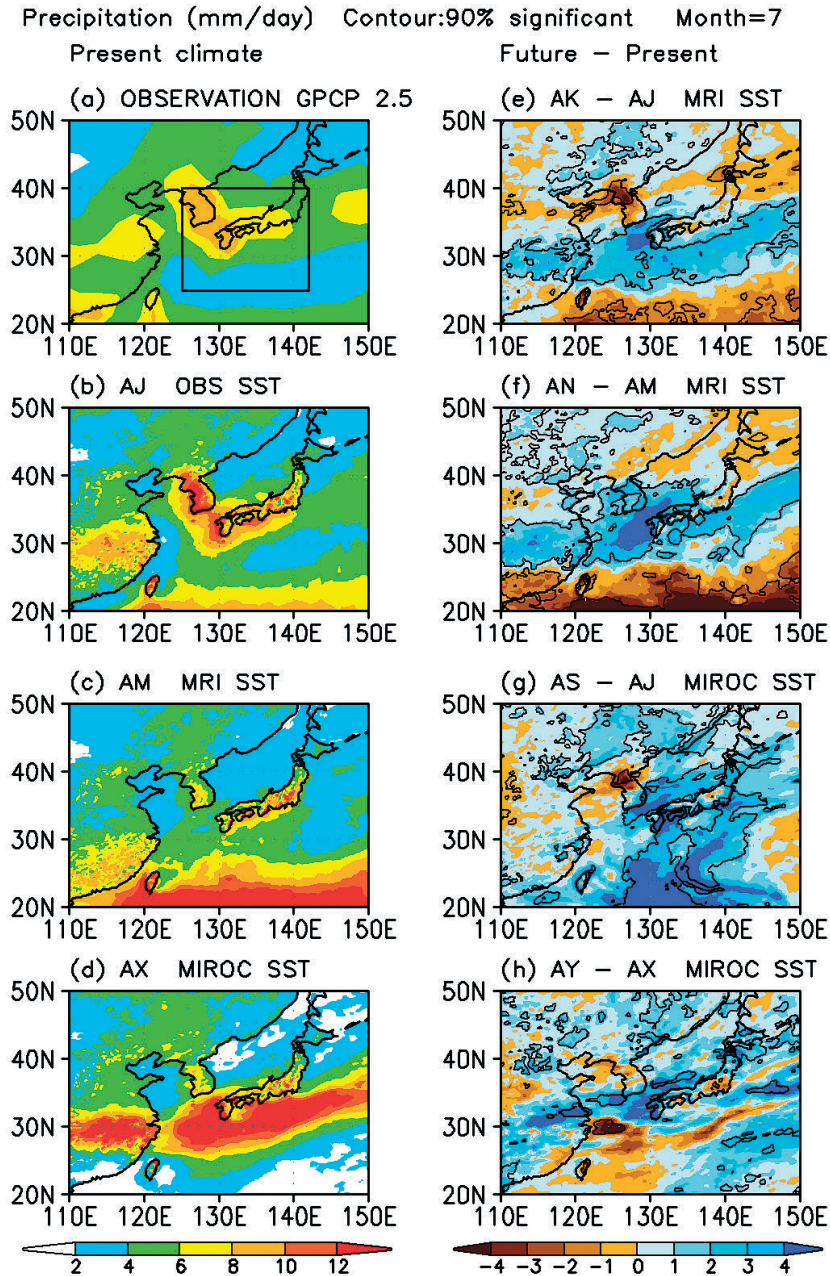


Fig. 4 Climatological precipitation for July (mm/day). (a) Observed precipitation by Global Precipitation Climatology Project (GPCP, Adler et al. 2003) averaged for 20 years from 1979 to 1998. Horizontal resolution is 2.5 degree. The black box shows the target region for Fig. 5. (b) Model's present climate simulation with observed SST (AJ). (c) Model's present climate simulation with MRI-CGCM2.3.2 SST (AM). (d) Model's present climate simulation with MIROC (hires) SST (AX). (e) Change as future minus present climate simulation (AK-AJ). Contours show a 90% significance. (f) AN-AM. (g) AS-AJ. (h) AY-AX.

(d), the timing and location of the Baiu rain band seem to be erroneous. Future changes (e-h) consistently show that precipitation increases from the end of July to the beginning of August around the latitudes 30-35N. This indicates that the termination of the Baiu season tends to be delayed until August, which is consistent with the report of Kusunoki et al. (2006).

2. Subproject 2: Development of non hydrostatic models (NHMs) with horizontal resolutions of several km

2.1 Changes of precipitation amount and intensity due to the global warming

Changes in precipitation due to the global warming projected by 5km-NHM are shown in Fig. 6. The precipitation amount over Japan is projected to increase, and the rate of

increase is estimated to be about 10%. In particular, the precipitation amount in the KS region reaches approximately 120% (Fig. 6a). On the other hand, precipitation in the EJ and NJ regions decreases by about 5%. The future precipitation change is mainly attributable to the changes in the horizontal transport of water vapor and its convergence associated with the intensification of a subtropical high (Kusunoki et al., 2006).

Another change in the precipitation property is the intensification of precipitation. The rates of increase of the precipitation frequency are larger with more intense precipitation. For example, the rate of increase (red line in Fig. 6b) is about 1.9 with an intensity of 30 mm/h in the KS region. The rate for intensities of 1 and 4 mm/h is from 0.9 to 1.2 (not shown).

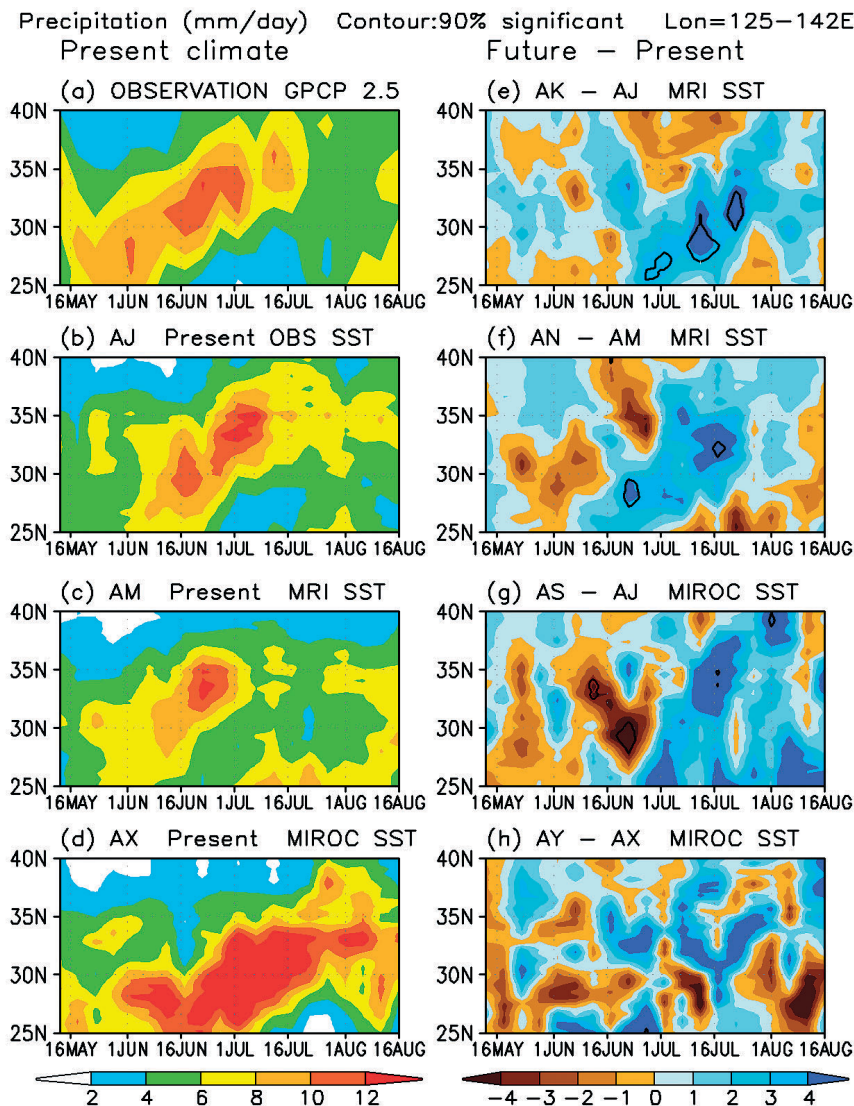


Fig. 5 Time evolution of pentad mean precipitation (mm/day) averaged for 125-142E. From pentad 27(11-15 May) to pentad 46 (14-18 Aug.). The target region is shown by the black box in Fig. 4a. (a) Observation by GPCP data as in Fig. 4a. (b) Model's present climate simulation with observed SST (AJ). (c) Model's present climate simulation with MRI-CGCM2.3.2 SST (AM). (d) Model's present climate simulation with MIROC (hires) SST (AX). (e) Change as future minus present climate simulation (AK-AJ). (f) AN-AM. (g) AS-AJ. (h) AY-AX. Contours show a 90% significance.

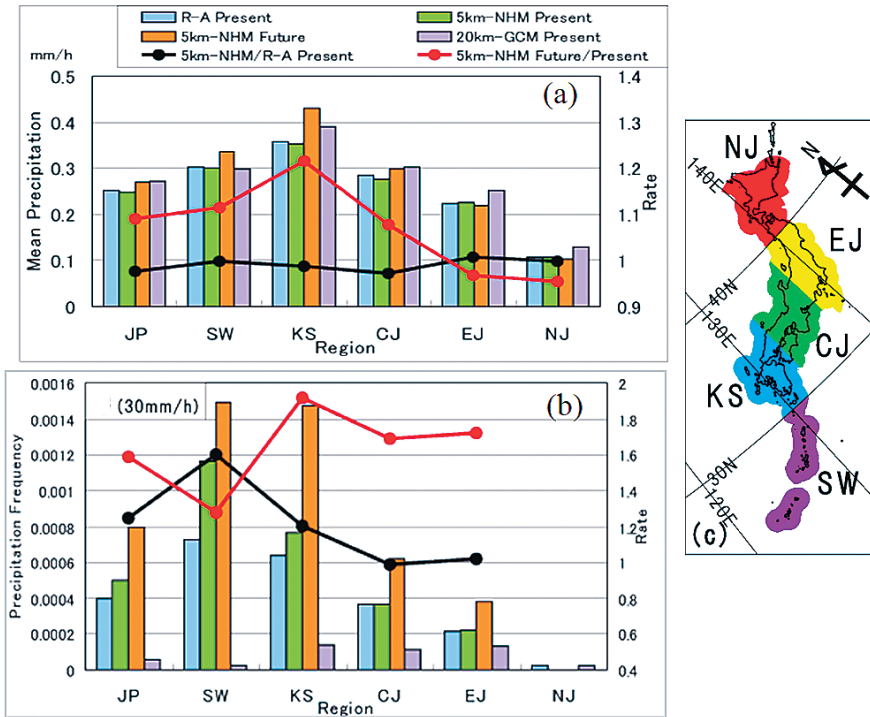


Fig. 6 (a) Mean precipitation amounts (mm/h) and (b) frequencies of heavy rainfall over Japan (all) and five regions in June and July. Five regions denoted by SW (Southwest), KS (Kyushu), CJ (Central Japan), EJ (Eastern Japan), and NJ are shown in (c). In (a) and (b), green and orange columns denote the 5km-NHM results in the present climate and the 5km-NHM results in the future warmer climate, respectively. The red line shows the increase rate due to global warming (Future climate/Present climate). The black line shows a ratio, 5km-NHM (Present climate) /R-A(Radar-AMeDAS precipitation data).

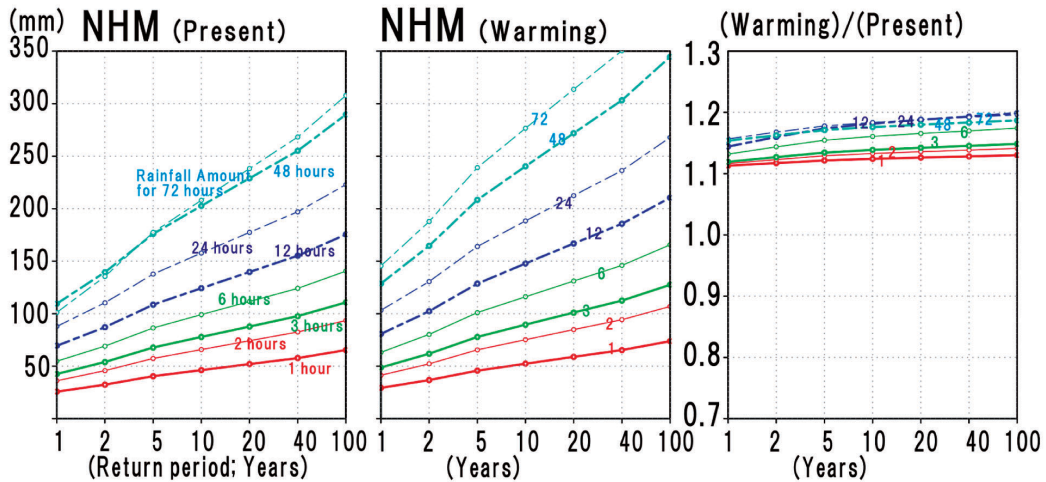


Fig. 7 Return values for 1, 2, 3, 6, 12, 24, 48, 72-hour precipitation as a function of return period over land in the western Japan, simulated by the 5km-NHM. (Left) present climate, (middle) global warming climate, (right) ratios of global warming climate to present one.

2.2 Extreme precipitation events

The changes of return values of extreme precipitation in the global warming climate simulated by the 5km-NHM are shown in Fig. 7. Here, the return value of extreme precipitation is defined as the rainfall intensity that occurs once every N year, assuming that the occurrence frequency is represented by a Gumbel distribution. In a warmer climate, the return values of extreme precipitation increase by about 10-20%.

2.3 Structure of Mesoscale Convective Systems (MCSs) in the global warming climate simulated by NHM

In a warmer climate, two types of MCSs appear in the vicinity of Kyushu Island. One travels from the Chinese Continent and the other from the southern part of the East China Sea to Kyushu Island. These two MCSs often merge over the sea southwest of Kyushu Island, and they rapidly develop to bring heavy precipitation to the vicinity of

Kyushu Island. Among the latter, MCSs with low cloud-tops of altitude below 4 km are found.

In comparison with the present climate, the averaged cloud and rain water mixing ratios in the vicinity of Kyushu Island become much larger, and the peak altitude of the mixing ratios are about 0.5-1.0 km higher in the global warming climate. The cloud water mixing ratio between the 2-4 km height increases in the global warming climate, corresponding to MCSs with low cloud-tops.

2.4 Experiment with 1km-NHM

Precipitation frequency spectrum (PFS) of 1km-NHM compared with that of 5km-NHM are shown in Fig. 8. The frequencies of moderate (intensities from 5 to 15 mm/h) precipitations increase and heavy (larger than 20 mm/h) precipitations decrease with 1km-NHM. This suggests that the 1km-NHM improves the inconsistency between the PFS of 5km-NHM and observation pointed out by Yoshizaki et al. (2005).

Figure 9 shows the distributions of the top values of 24-hour-accumulated precipitation amounts (24h-Top) averaged over a horizontal grid size of 20 km that is calculated from a 15-day experiment data. Many grids of the 24h-Top that are larger than 300 mm/day are found in the 5km-NHM experiment (Fig. 9a), while the peak value of the 24h-Top is about 200 mm/day in the 20km-GCM experiment (Fig. 9c).

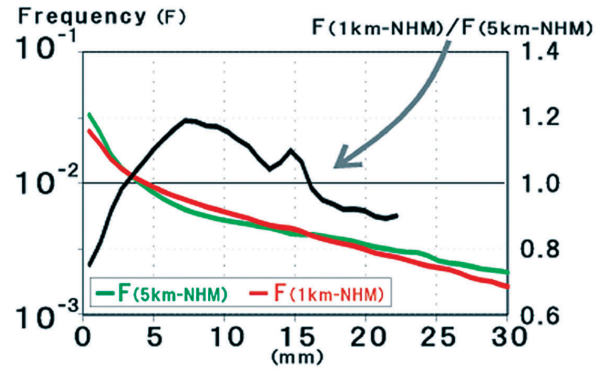


Fig. 8 Precipitation frequencies of 5km- (green line) and 1km-NHM (red line) against one-hour precipitation intensity. These are calculated from a 15-day data set of a year in the present climate over an area of 122-135E, 27-35N. The black line indicates a ratio of 1km-NHM to that of 5km-NHM.

Moreover, in the 1km-NHM experiment (Fig. 9b), a band-shaped cluster of the 24h-Top larger than 400 mm/day is seen over the central portion of the Kyushu District. The band-shaped precipitation system is similar to that reported by Kato (1998), which is maintained by the back-building-type process. The organized precipitation systems are often observed and sometimes cause extremely heavy precipitation events. Therefore, high-resolution experiments, such as that with 1km-NHM, and statistical investigations with regard to the dependency on the grid size might be required.

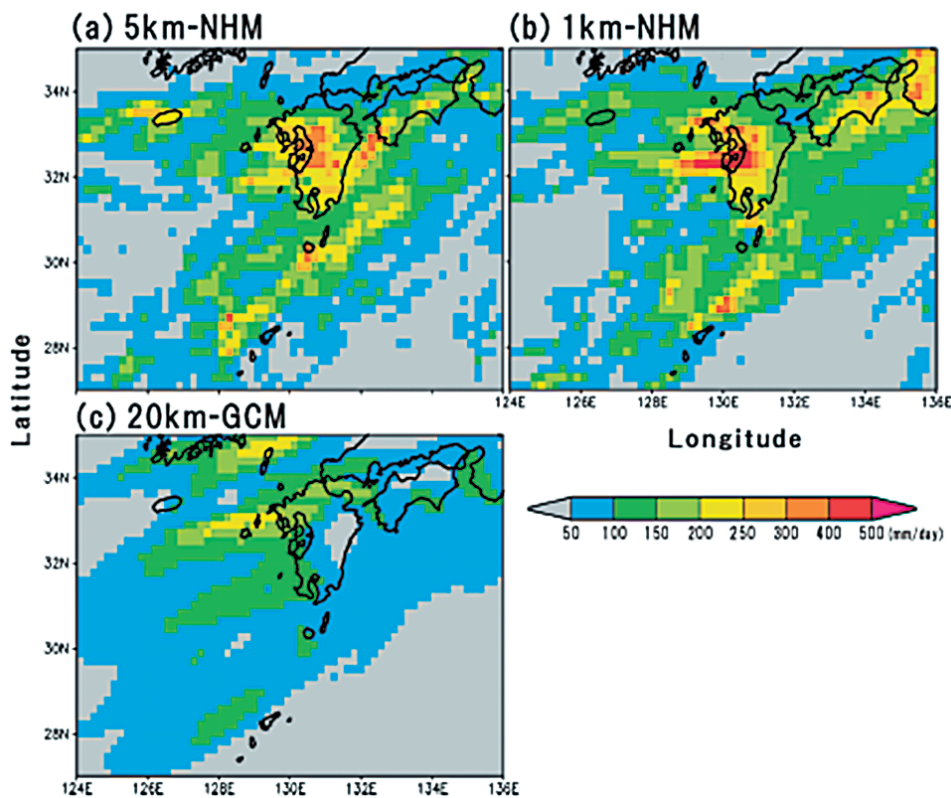


Fig. 9 Distributions of the top values of 24-hour-accumulated precipitation amounts (24h-Top) for (a) 5km-NHM, (b) 1km-NHM, and (c) 20km-GCM. These are selected from a 15-day data set as an example.

Bibliographies

- Adler, R. F., G. J. Huffman, A. Chang, R. Ferrano, P.-P. Xie, J. Janowiak, B. Rudolf, U. Schneider, S. Curtis, D. Bolvin, A. Gruber, J. Susskind, P. Arkin and E. Nelkin, 2003: The Version-2 Global Precipitation Climatology Project (GPCP) Monthly Precipitation Analysis (1979–Present). *J. Hydrometeorol.*, **4**, 1147–1167.
- Bengtsson, L., M. Botzet and M. Esch, 1996: Will greenhouse gas-induced warming over the next 50 years lead to higher frequency and greater intensity of hurricanes? *Tellus*, **48A**, 57–73.
- IPCC, 2000: Special Report on Emissions Scenarios. A Special Report of Working Group III of the Intergovernmental Panel on Climate Change. [Nakić enović, N., J. Alcamo, G. Davis, B. de Vries, J. Fenhann, S. Gaffin, K. Gregory, A. Grübler, T. Yong Jung, T. Kram, E. L. La Rovere, L. Michaelis, S. Mori, T. Morita, W. Pepper, H. Pitcher, L. Price, K. Riahi, A. Roehrl, H.-H. Rogner, A. Sankovski, M. Schlesinger, P. Shukla, S. Smith, R. Swart, S. van Rooijen, N. Victor and Z. Dadi (eds.)]. Cambridge University Press, Cambridge, UK.
- IPCC, 2001: Climate Change 2001: The Scientific Basis. Contribution of Working Group I to the Third Assessment Report of the Intergovernmental Panel on Climate Change [Houghton, J. T., Y. Ding, D. J. Griggs, M. Noguer, P. J. van der Linden, X. Dai, K. Maskell and C. A. Johnson (eds.)]. Cambridge University Press, Cambridge, United Kingdom and New York, NY, USA, 881pp.
- Kanada, S., C. Muroi, Y. Wakazuki, K. Yasunaga, A. Hashimoto, T. Kato, K. Kurihara, M. Yoshizaki, A. Noda, 2005: Structure of mesoscale convective systems during the late Baiu season in the global warming climate simulated by a non-hydrostatic regional model. *SOLA*, **1**, 117–120.
- Kato, T., 1998: Numerical simulation of the band-shaped torrential rain observed over southern Kyushu, Japan on 1 August 1993. *J. Meteor. Soc. Japan*, **76**, 97–128.
- Kusunoki, S., J. Yoshimura, H. Yoshimura, A. Noda, K. Oouchi and R. Mizuta, 2006: Change of Baiu rain band in global warming projection by an atmospheric general circulation model with a 20-km grid size. *J. Meteor. Soc. Japan*, **84**, 581–611.
- Michaelis, S. Mori, T. Morita, W. Pepper, H. Pitcher, L. Price, K. Riahi, A. Roehrl, H.-H. Rogner, A. Sankovski, M. Schlesinger, P. Shukla, S. Smith, R. Swart, S. van Rooijen, N. Victor and Z. Dadi (eds.)]. Cambridge University Press, Cambridge, UK.
- Mizuta, R., K. Oouchi, H. Yoshimura, A. Noda, K. Katayama, S. Yukimoto, M. Hosaka, S. Kusunoki, H. Kawai and M. Nakagawa, 2006: 20-km-mesh global climate simulations using JMA-GSM model -- mean climate states --. *J. Meteor. Soc. Japan*, **84**, 165–185.
- Oouchi, K., J. Yoshimura, H. Yoshimura, R. Mizuta, S. Kusunoki and A. Noda, 2006: Tropical cyclone climatology in a global-warming climate as simulated in a 20km-mesh global atmospheric model: Frequency and wind intensity analyses. *J. Meteor. Soc. Japan*, **84**, 259–276.
- Sugi, M., A. Noda and N. Sato, 2002: Influence of the Global Warming on Tropical Cyclone Climatology: An Experiment with the JMA Global Model. *J. Meteor. Soc. Japan*, **80**, 249–272.
- Yoshimura, H. and T. Matsumura, 2005: CAS/JSC WGNE Research Activities in Atmospheric and Ocean Modeling, **35**, 3.27–28.
- Yoshizaki, M., C. Muroi, S. Kanada, Y. Wakazuki, K. Yasunaga, A. Hashimoto, T. Kato, K. Kurihara, A. Noda and S. Kusunoki, 2005: Changes of Baiu (Meiyu) frontal activity in the global warming climate simulated by a non-hydrostatic regional model. *SOLA*, **1**, 25–28.
- Yukimoto, S., A. Noda, T. Uchiyama, S. Kusunoki, and A. Kitoh, 2006: Climate changes of the twentieth through twenty-first centuries simulated by the MRI-CGCM2.3. *Pap. Meteor. Geophys.* **51**, 51–96.

高精度・高分解能気候モデルの開発

プロジェクト責任者

野田 彰 気象研究所

著者

野田 彰*¹, 楠 昌司*¹, 中村 誠臣*¹

*¹ 気象研究所

文部科学省「人・自然・地球共生プロジェクト」の第4課題として、地球シミュレータに最適化された高精度・高分解能気候モデルを開発し、地球温暖化が熱帯低気圧、梅雨前線、集中豪雨など、これまでの気候モデルではシミュレート出来なかった現象に及ぼす影響を明らかにした。

20km格子全球大気大循環モデルを使用し、タイムスライス法による地球温暖化予測実験を行った。タイムスライス法は、大気海洋結合モデルによる海面水温(SST)予測を用いて、20km全球大気モデルのような高解像度の大気モデルを強制する方法である。現在気候では、異なったSSTを用いて4種類の実験を行った。ATでは年々変動のある観測されたSSTを、AJでは気候値SSTを与えた。AMは気象研究所大気海洋結合モデルMRI-CGCM2.3.2のSSTを、AXは大気海洋結合モデルMIROCのSSTを与えた。将来気候は、IPCCの温室効果気体排出シナリオA1Bを仮定した。AKは、観測された気候値SSTにMRI-CGCM2.3.2によって予測されたSST変化を上乗せした。ASは、同様にMIROCによって予測されたSST変化を上乗せした。AMはMRI-CGCM2.3.2によって予測されたSSTそのものを用いた。AXはMIROCによって予測されたSSTそのものを用いた。実行した8つの実験は、SSTの年々変動のある実験(AT, AM, AN, AX, AY)とSSTの年々変動の無い実験(AJ, AK, AS)に分類される。

20kmメッシュ全球大気気候モデルによる一連の数値実験結果を解析することにより、これまでの研究で得られている地球温暖化時の熱帯低気圧の変化傾向がどれほど強固なものであるかを調べた。いずれの地球温暖化実験においても、全球スケールおよび半球スケールにおいて熱帯低気圧の発生数は顕著に減少した。また、熱帯低気圧を強度別に解析した結果、海上/地上での最大風速が50 m/sを超えるような強い熱帯低気圧はいずれの温暖化実験でも増加しており、この傾向は全球的に海面水温が高い条件の実験ではより顕著であった。これらの結果はこれまでの研究を支持するものである。海域スケールでの熱帯低気圧発生数については、海面水温の設定方法により変化傾向が異なる場合があったが、モデルの現在気候の再現性、大気モデルによるタイムスライス実験と大気海洋結合モデルによる温暖化予測実験の整合性に留意することにより、海域スケールの変化傾向についても予測できる可能性があると考えられる。

梅雨については、AK, AM, AS, AXのいずれの実験も中国大陸の揚子江付近、東シナ海、日本の南海上で降水量が増加する。一方、朝鮮半島、日本海、北日本では降水量の変化傾向が実験によって異なった。梅雨明けが8月にまで遅れる傾向は、どの実験でも顕著であった。

地球シミュレーター上で最適化された非静力学モデルを開発し、20km格子全球大気大循環モデルにネステイングして、現在気候・将来気候(地球温暖化時)のそれぞれ10年間について、水平解像度5kmによる梅雨期のシミュレーションを実施した。その結果、温暖化時には、梅雨期の降水量が北・東日本を除いて増加すること、強度の強い降水ほど発生頻度が増大すること、極端降水の再現期待値が1、2割程度増大するなどがわかった。更に、降水現象をより詳細に調べるとともに解像度の影響を調べるため、解像度1kmのNHMを使って、降水の多かった7月を対象としてシミュレーションを行った。その結果、1km-NHMは強度別の降水頻度スペクトルの表現において5km-NHMの結果を改善すること、降水系の組織化による降水の集中を5km-NHMに比べて良く表現することなどがわかった。

キーワード：地球温暖化予測, 高分解能全球大気モデル, 雲解像モデル, 梅雨, 台風